SUPPLEMENTARY INFORMATION

High-throughput Light-induced Immunoassay with Milliwatt-level Laser under One-minute Optical Antibody-coating on Nanoparticle-imprinted Substrate

Masatoshi Kanoda[1,2,3], Kota Hayashi[1,2,3], Yumiko Takagi[2], Mamoru Tamura[2,4], Shiho Tokonami[2,3,#*], and Takuya Iida[1,2,#*]

[1]Department of Physics, Graduate School of Science, Osaka Metropolitan University, 1-2 Gakuencho, Nakaku, Sakai, Osaka 599-8570, Japan

[2]Research Institute for Light-induced Acceleration System (RILACS), Osaka Metropolitan University, 1-2 Gakuencho, Nakaku, Sakai, Osaka 599-8570, Japan

[3]Department of Applied Chemistry, Graduate School of Engineering, Osaka Metropolitan University, 1-2 Gakuencho, Nakaku, Sakai, Osaka 599-8570, Japan

[4]Department of Materials Engineering Science, Graduate School of Engineering Science, Osaka University, 1-3 Machikaneyama-cho, Toyonaka, Osaka 560-8531, Japan

*Corresponding Authors: t-iida@omu.ac.jp (T.I.); tokonami@omu.ac.jp (S.T.)

#These authors contributed equally to this work.

Movie Legends:

Please refer to the detail in the main text.

Movie S1. Video (real time) of light-induced assembly of green fluorescent nanoparticles (100 nm in diameter) via 60 seconds laser irradiation on a nanoparticle-imprinted plasmonic substrate (NPI-PS). Laser irradiation was started at 5 seconds and stopped 65 seconds after the video started.

Supplementary Figures:

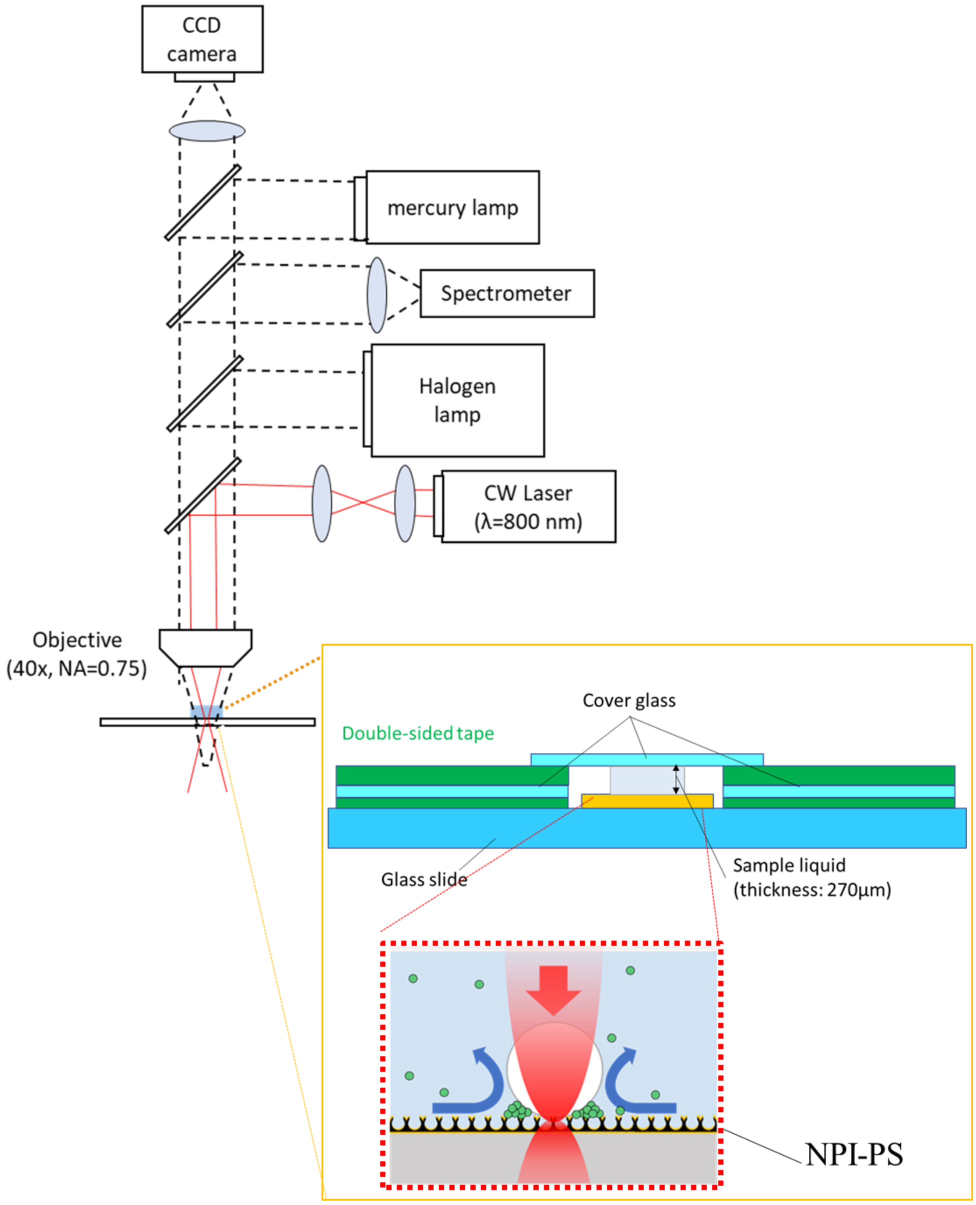

Fig. S1 Optical system used in experiments of optical condensation.
Sample liquid was dropped onto a nanoparticle-imprinted plasmonic substrate (NPI-PS) on the glass slide and confined with cover glass, where the height of liquid was adjusted by double-stick tapes sandwiching cover glasses at the both sides.

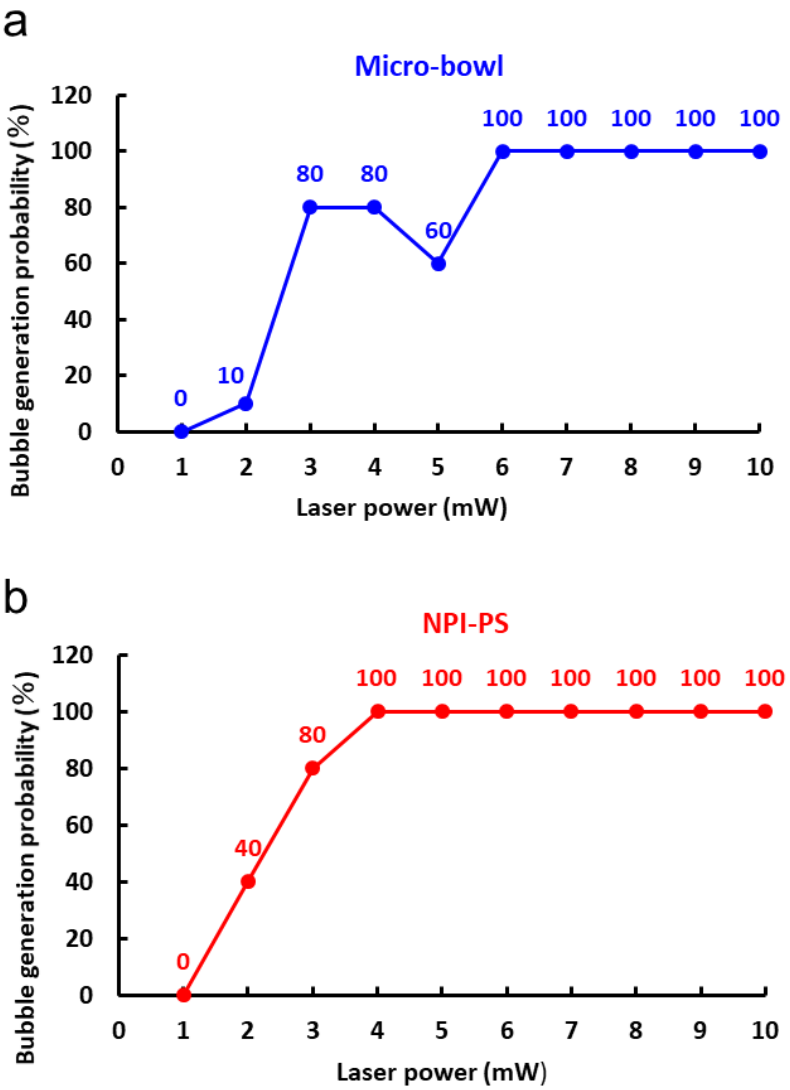

Fig. S2 Comparison of bubble generation probability between micro-bowl substrate and nanoparticle-imprinted plasmonic substrate (NPI-PS).

a. Relationship between the probability of bubble generation and laser power by micro-bowl.

b. Relationship between the probability of bubble generation and laser power by NPI-PS.

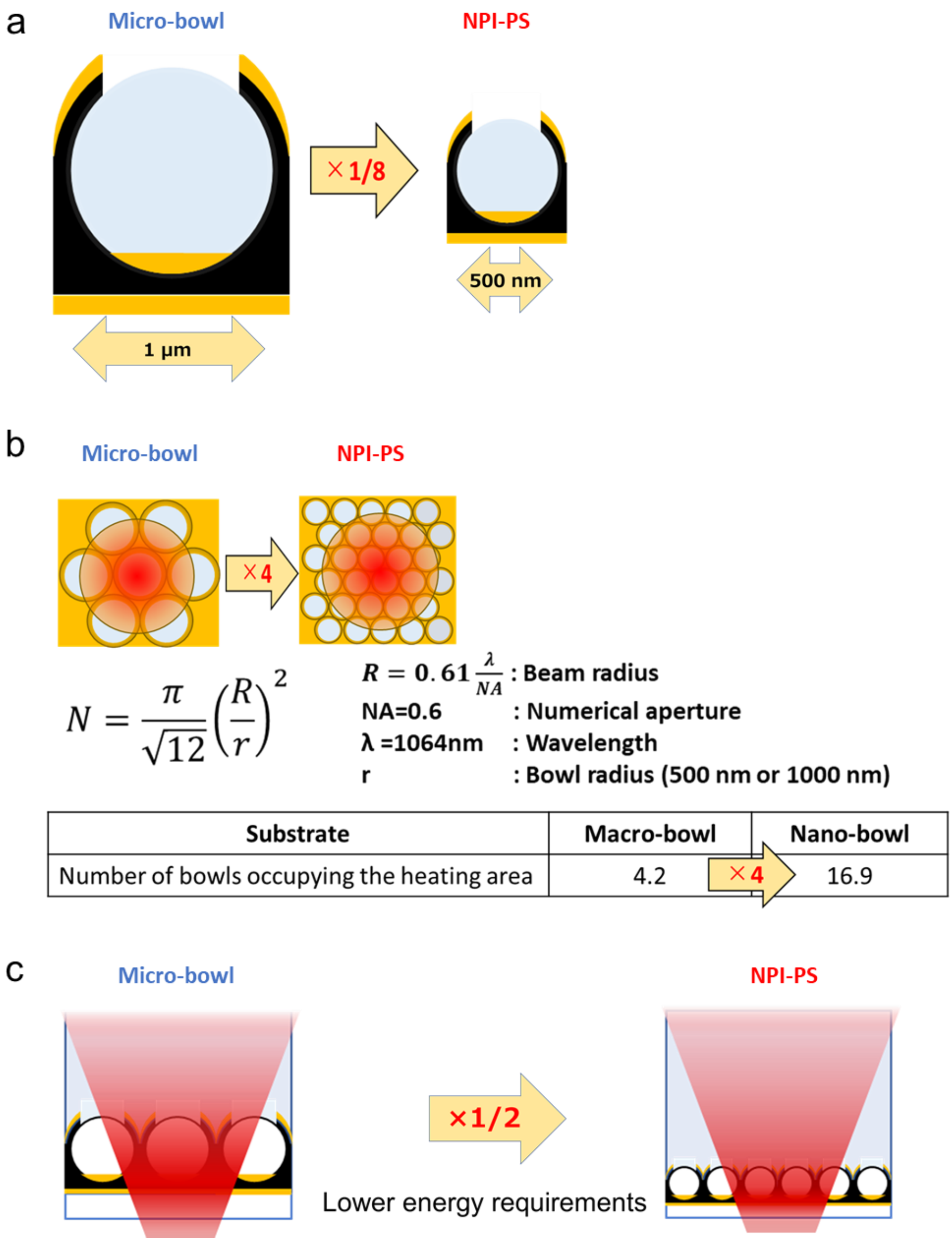

Fig. S3 Mechanism of highly efficient light-induced bubble generation.
a. Comparison of the amount of air held by one bowl structure.
b. Comparison of the number of bowl structures entering the laser point
c. Comparison of heat generation efficiency between NPI-PS and micro-bowl.

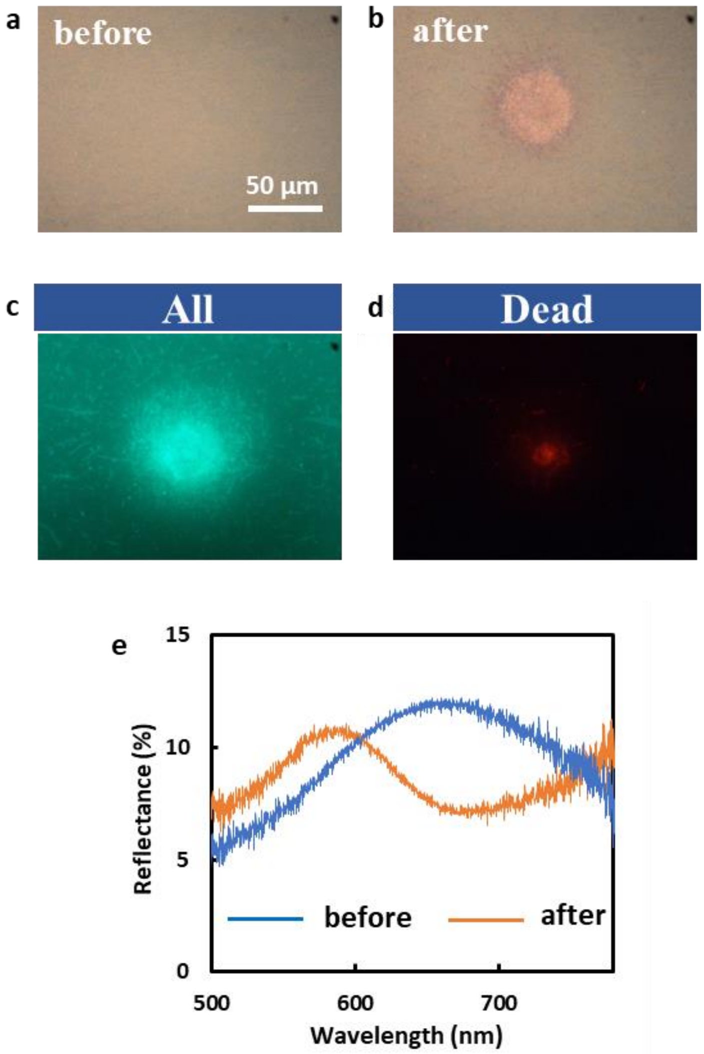

Fig. S4 Optical condensation of *Escherichia coli* (4.0 × 10^8 CFU/mL, stained using SYTE9 and PI) with NPI-PS.

a. NPI-PS before optical condensation.

b. NPI-PS after optical condensation

c. Fluorescence image of assembled *E. coli*.

d. Fluorescence image of damaged *E. coli* among the assembled individuals.

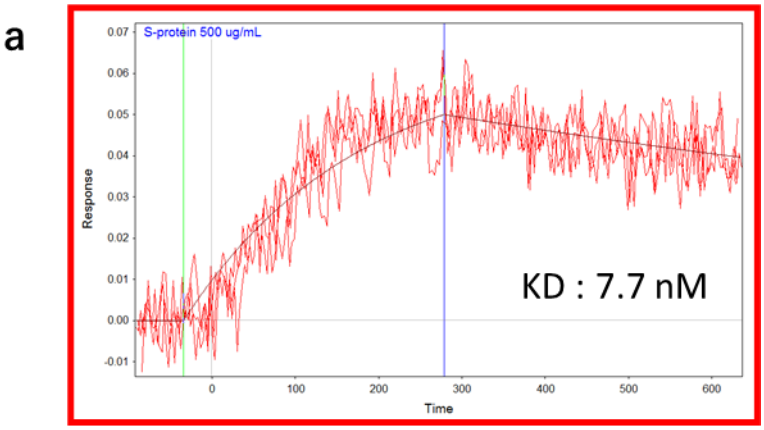

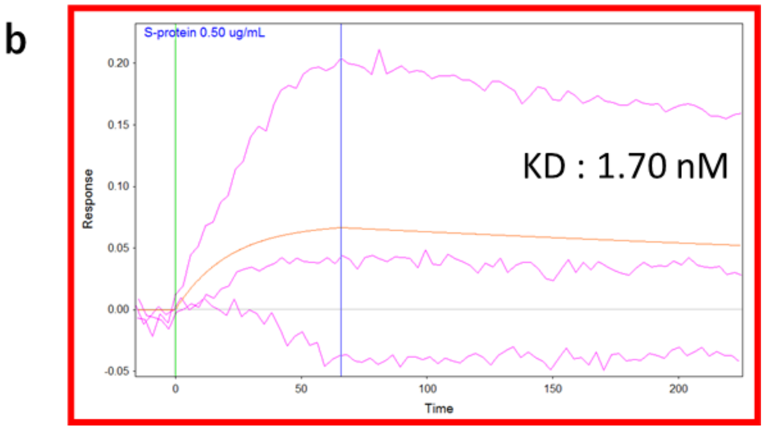

Fig. S5 KD values for coronavirus-derived S-protein and antibodies.

a. KD values for the S-protein and anti-S1 antibody.

b. KD values for the S-protein and anti-S2 antibody.

These KD values were observed with SPR molecular interaction analyzer (OpenPlexTC-OHU, Horiba, Japan).

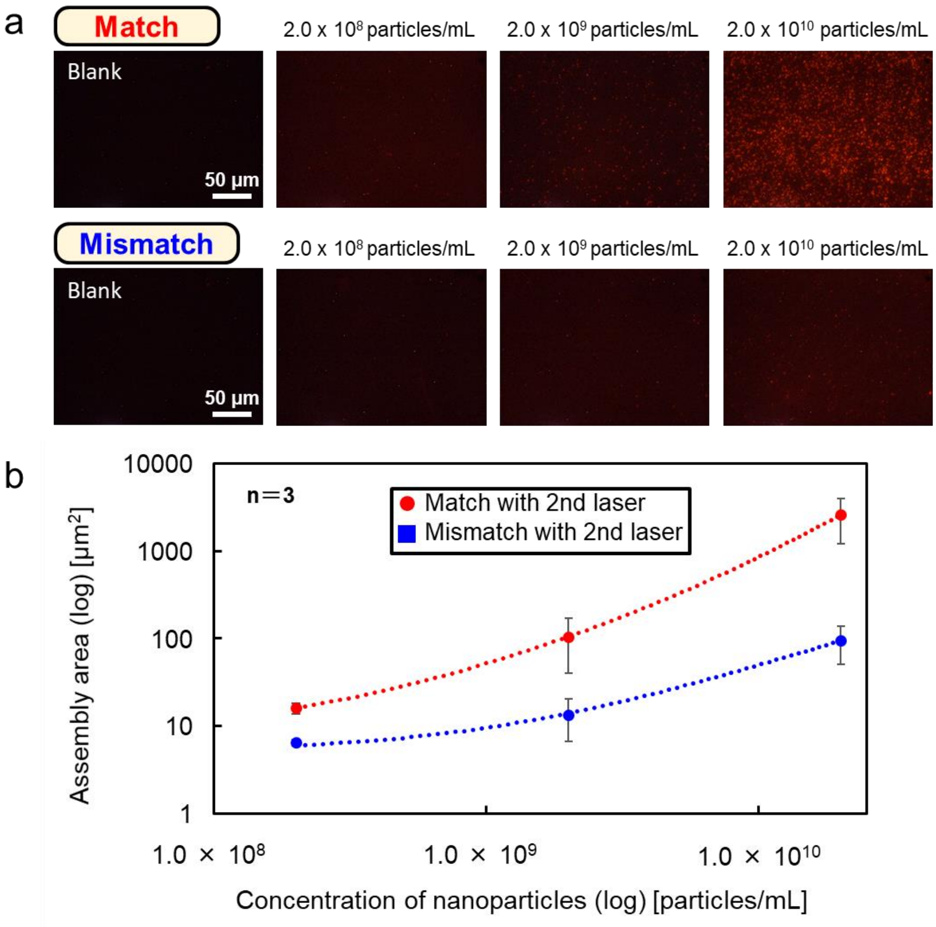

Fig. S6 Detection of virus-mimicking nanoparticles (VMNPs) using a nanoparticle-imprinted plasmonic substrate (NPI-PS) in an artificial saliva mixture.

a. Fluorescence images of VMNPs (match) and unmodified nanoparticles (mismatch) at different concentrations after optical condensation with the dispersion liquid containing 50 % of artificial saliva under the same condition in Fig. 3b.

b. Relationship between assembly area and concentration of nanoparticles for VMNPs (match, red plots) and unmodified nanoparticles (mismatch, blue plots), where the averaged assembly area was calculated via fluorescence image from Fig. S6a for n=3. Error bars indicate standard deviation. The assembly area for 0 particles/mL (blank) was evaluated as 5.09 $\mu m^2 \pm 0.74$.

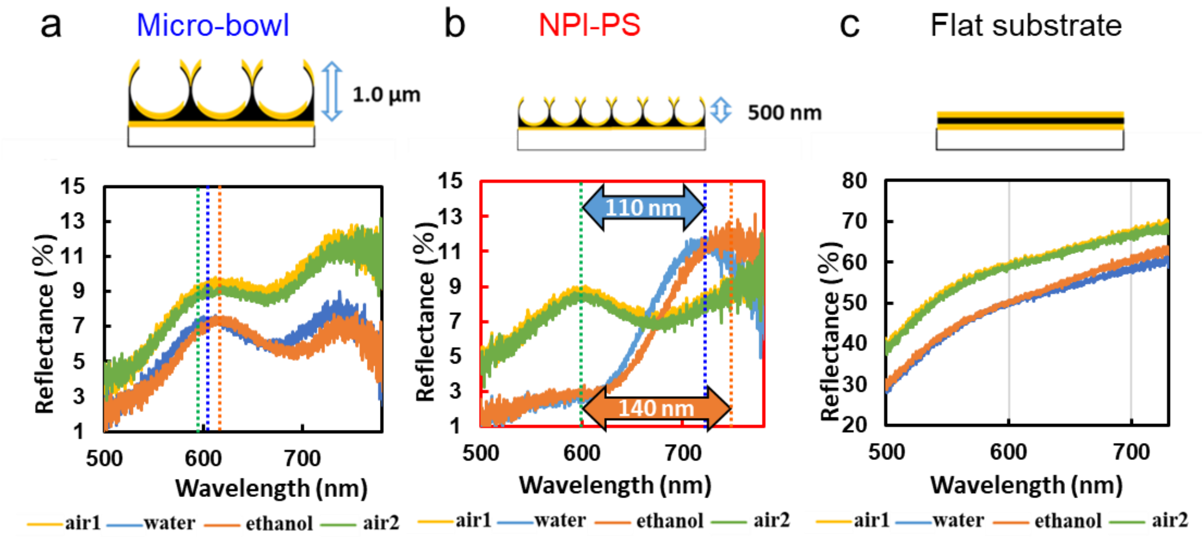

Fig. S7 Comparison between the optical responses of NPI-PS and micro-bowl substrate.

a. Reflectance spectra of micro-bowl in different media (air, water, ethanol).

b. Reflectance spectra of NPI-PS in different media (air, water, ethanol).

c. Reflectance spectra of flat substrate in different media (air, water, ethanol).

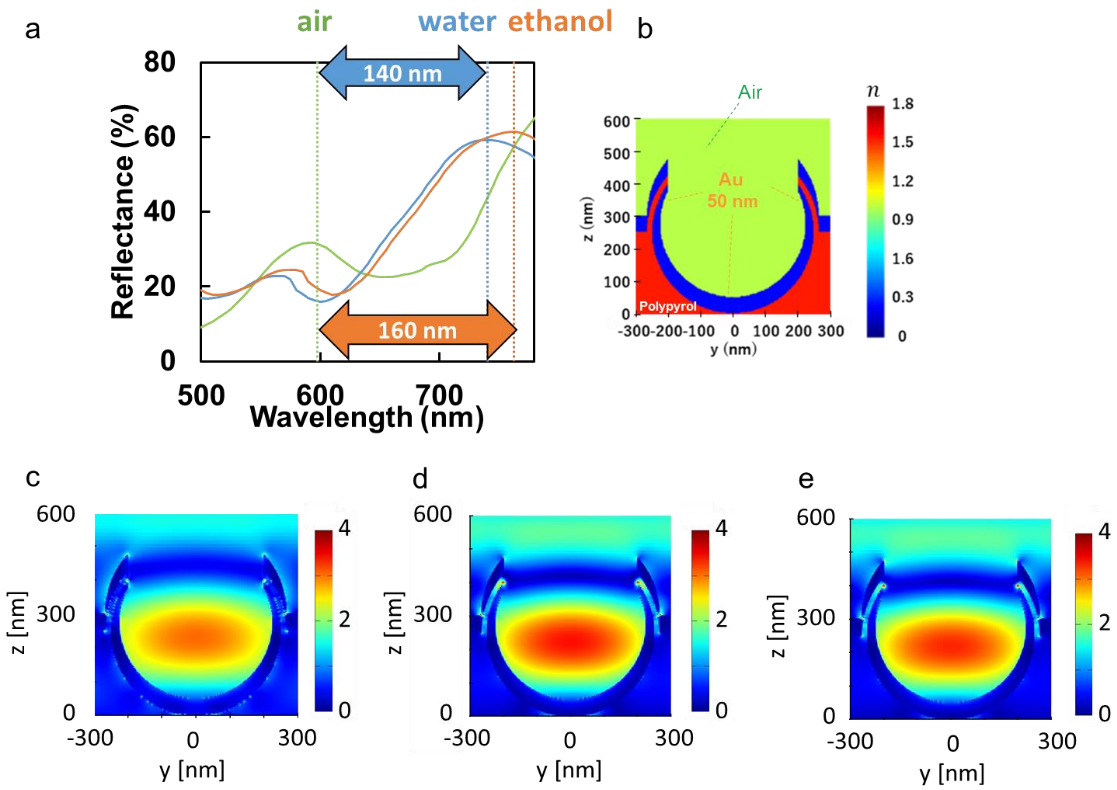

Fig. S8 Theoretical analysis of the optical responses of NPI-PS.

a. Reflectance spectra of NPI-PS in different media (air, water, ethanol).

b. Model for the calculation. Reflectance spectra of NPI-PS in different media;

c. air (refractive index: 1.00, wavelength: 600 nm),

d. water (refractive index 1.33, wavelength: 740 nm),

e. ethanol (refractive index: 1.36, wavelength: 760 nm).

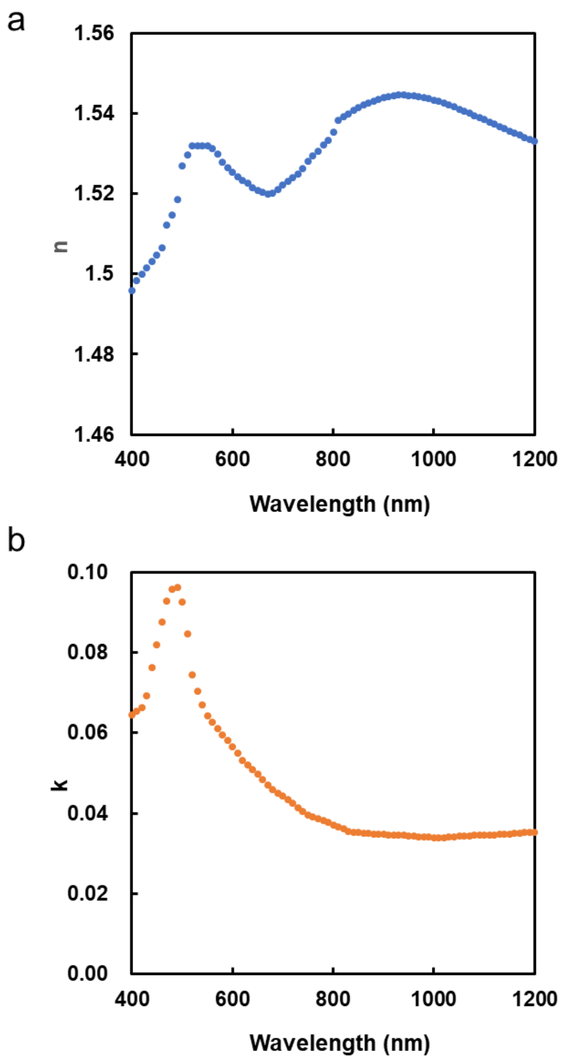

Fig. S9 Real and imaginary parts of refractive index of polypyrrole.

a. Real part and **b**. imaginary part of refractive index extracted from the experimental data in Ref. 38 (A. Ashery, et al., Synthetic Metals, 162, 1357 (2012).)